2nd International Conference on the Material Point Method for Modelling Soil-Water-Structure Interaction

Anura3D
MPM Research Community

Paper number: mpm2019.12
www.anura3d.com
www.mpm2019.eu

Soil-structure interaction simulation of landslides impacting a structure using an implicit material point method

Bodhinanda Chandra[1,*], Antonia Larese[2], Ilaria Iaconeta[2], Riccardo Rossi[2], Roland Wüchner[1,3]
[1]Department of Civil, Geo, and Environmental Engineering, Technical University of Munich, Munich, Germany
[2]International Center for Numerical Methods in Engineering, Technical University of Catalonia (UPC), Barcelona, Spain
[3]Chair of Structural Analysis, Technical University of Munich, Munich, Germany

[*] E-mail: bodhinanda.chandra@tum.de

ABSTRACT

Global warming and climate changes have been one of the many causes that triggered numerous catastrophic landslide and mudflow disasters in the past twenty years. The increase of earth temperature has contributed to the increase of precipitation and undisputedly affected the soil slope stability, which by further may cause landslides in various scale and speed. This large soil deformation phenomenon carries along huge rocks and heavy materials that often results in extensive damage in civil infrastructures both directly or indirectly. Coming with this motivation, a soil-structure interaction simulation based on the implicit material point method (MPM) has been implemented within the Kratos Multiphysics framework for the objective of predicting structural deformation and, furthermore, structural failure caused by environmental flow problems such as landslides. In the current study, the soil is modeled using a non-associated Mohr-Coulomb-based elastoplastic law, while the structure is modeled as elastic and Neo-Hookean hyperelastic materials. In the numerical tests conducted, the equivalent stress and displacement measured on both *rigid* and *flexible* structures show a good qualitative agreement. In the future works, a more adequate consideration of the soil and structural model will be investigated before conducting a real-scale landslide simulation.

KEY WORDS: material point method, nonlinear FEM, implicit MPM, soil-structure interaction, monolithic coupling

INTRODUCTION

In recent years, natural hazards involving large mass movements such as landslides, debris flows, and mudslides have significantly increased in frequency due to the influence of global warming and climate change (Kundzewicz et al., 2014; Goudie, 2006). These phenomena are extremely dangerous and often bring huge losses of lives and properties, resulting in a great economic loss, in particular, in rainy mountainous regions (Petley, 2012). In order to understand and predict the large soil movement and their effects on civil structures, analytical solutions to the model equations are impossible to obtain, whereas laboratory experiments are often limited in scope and scale, and thus, numerical methods may be employed due to its efficiency and convenience.

In this study, the dynamic impact load caused by landslides onto the structure is selected as a target issue and it is numerically represented by using a fully-implicit formulation of Material Point Methods (MPM). Introduced by (Sulsky et al., 1994; Sulsky et al., 1995) as the extension of Particle-In-Cell (PIC) method (Harlow, 1964), the MPM has gained a remarkably increasing popularity due to its capability in simulating solid mechanics problems which involve historically dependent materials and large deformations. As one of the fully Lagrangian particle methods which combines the strengths of Eulerian and Lagrangian methods, MPM has been utilized in various civil engineering applications, mostly in the analysis of moving discontinuities and large deformation systems such as the free-surface environmental flows with breaking, splash, and fragmentation; those which are difficult to simulate by using traditional FEM due to its mesh distortion issues. The method stores the historically changing variables and the material information at the moving particles, the so-called *material points* (MP), and uses a constantly-reset *background mesh* to solve the linear system of equations.

The objective of this study is to develop an accurate implicit MPM scheme to simulate natural hazards involving flows with particles of different sizes and their interaction and damaging effects on structures, in which can serve

with protective or non-protective function. With few notable exceptions (Guilkey & Weiss, 2003, Wang et al., 2016), the majority of the MPM algorithms are written assuming an explicit scheme (Bandara et al., 2015, Huang et al., 2008), in particular, for the simulation of mass movements and landslides (Soga et al., 2015, Andersen & Andersen, 2010, Mast, 2013). While this approach is generally favorable to simulate fast transient problems, the other alternative approach, which is the implicit formulation, is often more optimal to simulate cases when the rate of deformation is small, or when the driving force is solely gravity. On top of that, the stability of the method (for properly chosen dissipative methods) does not depend on the wave propagation speed within the media, and thus, allows the usage of a relatively larger time increment. This scheme can also be extremely advantageous to solve a Multiphysics coupling problems such as the soil-structure interaction (SSI) or when being coupled with FEM or other implicit-based methods.

The MPM code employed in the current research work has been developed by the authors within the Kratos Multiphysics open source platform (Dadvand, 2007; Dadvand et al., 2010) which details can be found in (Iaconeta et al., 2016, 2017, 2018). The code proposed is designed for an easy implementation and coupling for a wide range of Multiphysics constitutive laws. Further development will be to include some more advanced and specific laws suitable for different kind of soil or structural conditions.

GOVERNING EQUATIONS

Strong Form

Consider a body $\mathcal{B}$, which occupies a region Ω of a three-dimensional Euclidean space $\mathcal{E}$, with a regular boundary $\partial\Omega$ in its reference configuration. A deformation of $\mathcal{B}$ is defined by a one-to-one mapping as:

$$\varphi : \Omega \to \mathcal{E} \tag{1}$$

This maps each point $\mathbf{p}$ to in the body $\mathcal{B}$ into a spatial coordinate $\mathbf{x}$ as:

$$\mathbf{x} = \varphi(\mathbf{p}) \tag{2}$$

which represents the location of $\mathbf{p}$ in the deformed configuration of $\mathcal{B}$. The region of $\mathcal{E}$ occupied by $\mathcal{B}$ in its deformed configuration is denoted as $\varphi(\Omega)$.

The governing equations, i.e. the mass and the momentum conservation equations, can be written as:

$$\frac{D\rho}{Dt} + \rho\nabla\cdot\mathbf{v} = 0 \qquad \text{in} \quad \varphi(\Omega) \tag{3}$$

$$\rho\mathbf{a} - \nabla\cdot\boldsymbol{\sigma} = \rho\mathbf{b} \qquad \text{in} \quad \varphi(\Omega) \tag{4}$$

where ρ is the material density, $\mathbf{b}$ is the volume acceleration, and $\boldsymbol{\sigma}$ is the symmetric Cauchy stress tensor. The kinematic variables $\mathbf{a}$ and $\mathbf{v}$, which are the second and the first material derivatives of displacement $\mathbf{u}$ are the acceleration, and velocity, respectively. The balance equations above are to be solved numerically in three-dimensional field considering the following Dirichlet and Neumann boundary conditions:

$$\begin{aligned} \mathbf{u} &= \bar{\mathbf{u}} \quad \text{on} \quad \varphi(\partial\Omega_D) \\ \boldsymbol{\sigma}\cdot\mathbf{n} &= \bar{\mathbf{t}} \quad \text{on} \quad \varphi(\partial\Omega_N) \end{aligned} \tag{5}$$

Weak Form and Linearization in Spatial Form

The momentum balance equation above can be written in the weak form by employing the Galerkin method, similar to the one done in standard FEM procedure (Zienkiewicz & Taylor, 1977). The L_2 inner product of Equation 4 is derived using an arbitrary test function $\mathbf{w}$, such that $\mathbf{w} = \{\mathbf{w} \in \mathcal{V} \,|\, \mathbf{w} = 0 \text{ on } \varphi(\Omega)\}$, where $\mathcal{V}$ is the space of virtual displacements. By using the divergence theorem the weak form of momentum balance can be

obtained and written as:

$$G(\mathbf{u},\mathbf{w}) = \int_{\varphi(\Omega)} \boldsymbol{\sigma} : (\nabla^S \mathbf{w}) \mathrm{d}v - \int_{\varphi(\Omega)} \rho(\mathbf{b}-\mathbf{a}) \cdot \mathbf{w} \mathrm{d}v - \int_{\varphi(\partial\Omega_N)} \bar{\mathbf{t}} \cdot \mathbf{w} \mathrm{d}a = 0, \quad \forall \mathbf{w} \in \mathcal{V} \tag{6}$$

Equation 6 is valid for any kind of strain definitions, including the infinitesimal one. Since, in the current work, strong material and geometric nonlinearities are involved, a linearization of the weak form is, therefore, necessary, and thus, the Newton-Raphson method, which is based on Taylor's theorem, is used to approximate the solution iteratively. The algorithms of the solving strategy implemented in MPM fashion are explained in detail by (Iaconeta et al., 2016, 2017, 2018) considering an implicit time integration scheme of the Newmark-beta method.

Soil-Structure Interaction Coupling

In implicit MPM formulation, the solutions Equation 6 in all active background elements are approximated at every time step by iteratively solving the linear system of equations as follow:

$$\mathbf{K}_{IK}^{\tan} \delta\mathbf{u}_K = -\mathbf{R}_I \tag{7}$$

where the subscript *I* and *K* indicate the nodal indices. Here, $\mathbf{K}^{tan}$ denotes the derived tangential stiffness matrix, which includes the static and dynamic components, and **R** is the residual form of Equation 6.

In the present work, the soil is modeled as a non-associated elastoplastic constitutive law assuming Mohr-Coulomb yield criterion as specified by (Clausen et al., 2007) and implemented using finite strain assumption. Here, a monolithic coupling between soil and structural elements is considered; i.e. the linear system of equations of both soil and structure is solved at the same time. Therefore, one can modify the Equation 7 above by separating the soil and structure components as:

$$\begin{bmatrix} \mathbf{K}_S & \mathbf{K}_{S\Gamma} & 0 \\ \mathbf{K}_{\Gamma S} & \mathbf{K}_{\Gamma\Gamma} & \mathbf{K}_{\Gamma St} \\ 0 & \mathbf{K}_{St\Gamma} & \mathbf{K}_{St} \end{bmatrix}_{IK}^{\tan} \begin{Bmatrix} \delta\mathbf{u}_S \\ \delta\mathbf{u}_\Gamma \\ \delta\mathbf{u}_{St} \end{Bmatrix}_K = -\begin{Bmatrix} \mathbf{R}_S \\ \mathbf{R}_\Gamma \\ \mathbf{R}_{St} \end{Bmatrix}_I \tag{8}$$

Here, the index *S*, *St*, and *Γ* indicate the soil, structure, and interface nodal components, respectively.

NUMERICAL TESTS

Granular Flow Validation Test

In the present work, preliminary numerical simulations are performed to validate the quality of the soil elastoplastic modeling using the implemented implicit MPM scheme. For this purpose, a granular column collapse simulation of non-cohesive soil is simulated according to the two-dimensional experiment conducted by (Bui et al., 2008). Here, linear structured triangular elements are used to initialize the MPs and as the background mesh. The structured mesh arrangement is chosen to avoid the irregularities of the generated MP's density, which, by further, improving the numerical solutions. The initial geometry of the simulation can be seen in detail in Figure 1, while the material and problem data used to run the simulations are specified in Table 1 and Table 2.

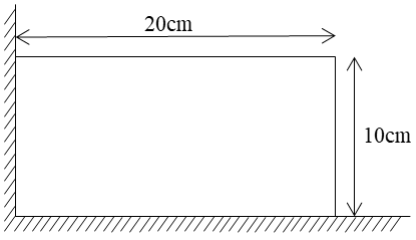

Figure 1 Granular flow validation. Geometry

In Figure 2, the obtained granular soil configuration is compared with the experimental data and the simulation results conducted in Smoothed Particle Hydrodynamics (SPH) by (Bui et al., 2008). One can observe that the obtained result shows a good agreement with the experimental measurement. However, there are still some differences, in particular, at the right-end region of the run-out surface. The authors believe that the quality of the results can be further improved, for example, by changing the constitutive model to more advanced laws or by introducing numerical damping as the standard Mohr-Coulomb model is said to be insufficient in simulating the inter-particle-collision energy dissipation as suggested by (Fern & Soga, 2016).

Table 1 Granular flow validation. Material data

Dimension	Density [kg/m^3]	Young's Modulus [kPa]	Poisson's ratio	Angle of internal friction[°]	Cohesion [kPa]	Dilatancy angle[°]
20cm×10cm	2650	840	0.3	19.8	0.0	0.0

Table 2 Granular flow validation. Problem data.

Element type	MP/cell	Mesh size [m]	Time step [s]
Triangle	3	0.002	0.00005

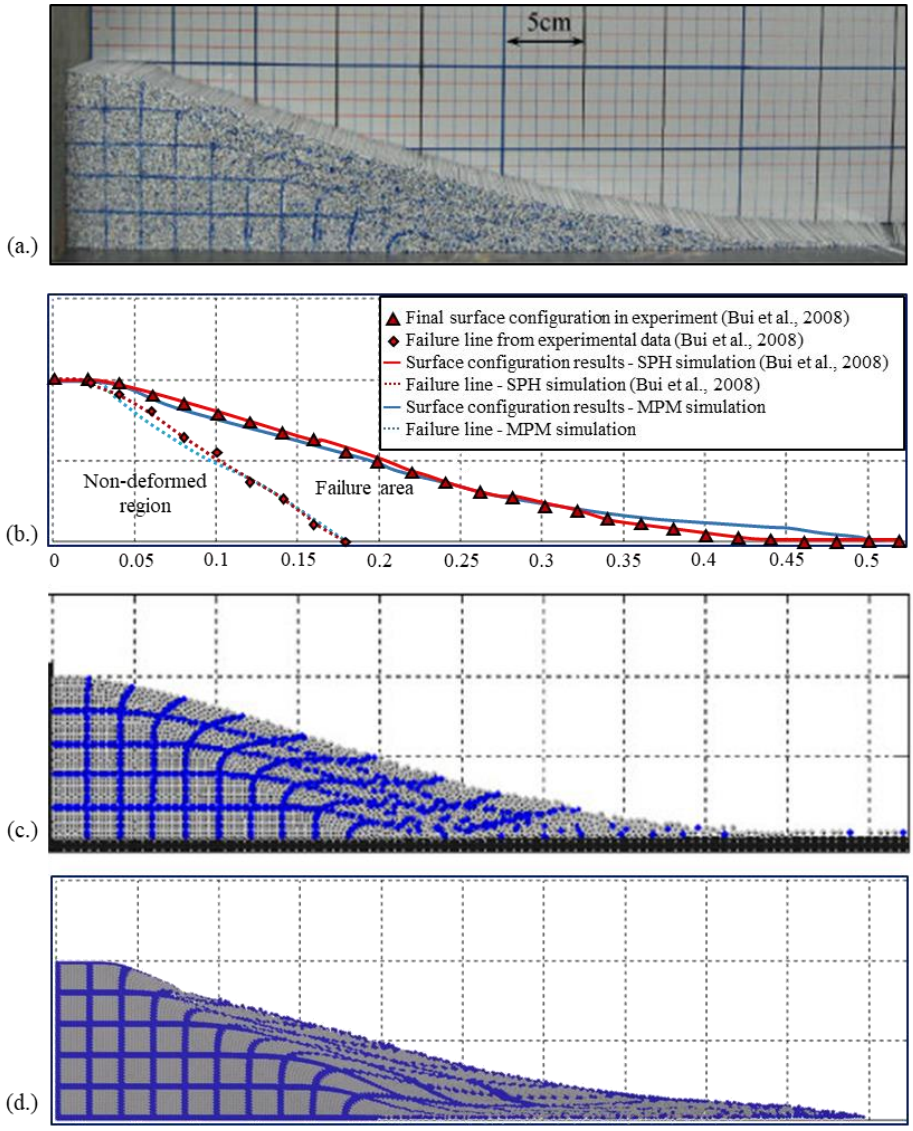

Figure 2 Granular flow validation. (a) Experiment conducted by (Bui et al., 2008), (b) comparison of final surface configuration and failure line, (c) simulation results of (Bui et al., 2008) by using SPH method, (d) simulation results obtained by implicit MPM method

Granular Flow Simulations with an Obstacle

A simple two-dimensional numerical simulation to test the implemented soil-structure interaction coupling scheme is presented. Here, a granular flow simulation using a similar model and material parameter to the previous validation test is performed after introducing a structural obstacle with a purpose to block the soil run-out as illustrated in Figure 3. In the present study, two types of materials are considered; one is a concrete-like structure, which will be referred as '*rigid*' from here on, with a linear-elastic assumption, and the other one is a '*flexible*' hyperelastic rubber-like material assuming a neo-Hookean model. The used structural constitutive models have been previously verified through several comparisons with analytical solutions, in particular, for solid beam problems. In order to check the simulation performance, a measurement point "A" is selected to measure the structural displacement upon the soil impact. The material data used to simulate the structural obstacle is specified in Table 3 and a mesh sensitivity analysis is carried out to understand how the mesh refinement affect the obtained results.

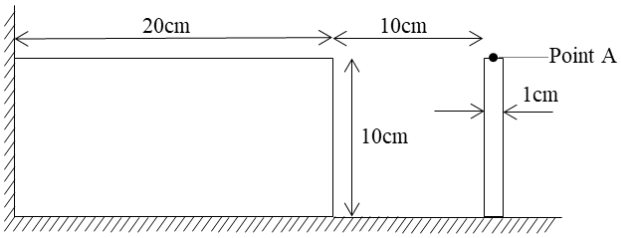

Figure 3 Granular flow simulations with an obstacle. Geometry

Table 3 Granular flow simulations with an obstacle. Material data of the obstacle.

	Material type	Density [kg/m^3]	Young's Modulus [MPa]	Poisson's ratio
a.)	Concrete-like (rigid)	2550	3×10^4	0.3
b.)	Rubber-like (flexible)	1100	1	0.0

In Figure 4 and 5, it can be observed that the simulation results show a very good qualitative result, simulating the equivalent stress of the obstacle structure and its convergence in displacement with respect to the conducted mesh study – this can be seen thoroughly in the flexible structure case. Unfortunately the current results are not yet validated with any experiments, and thus, further verification and validation test are planned to be performed in the near future.

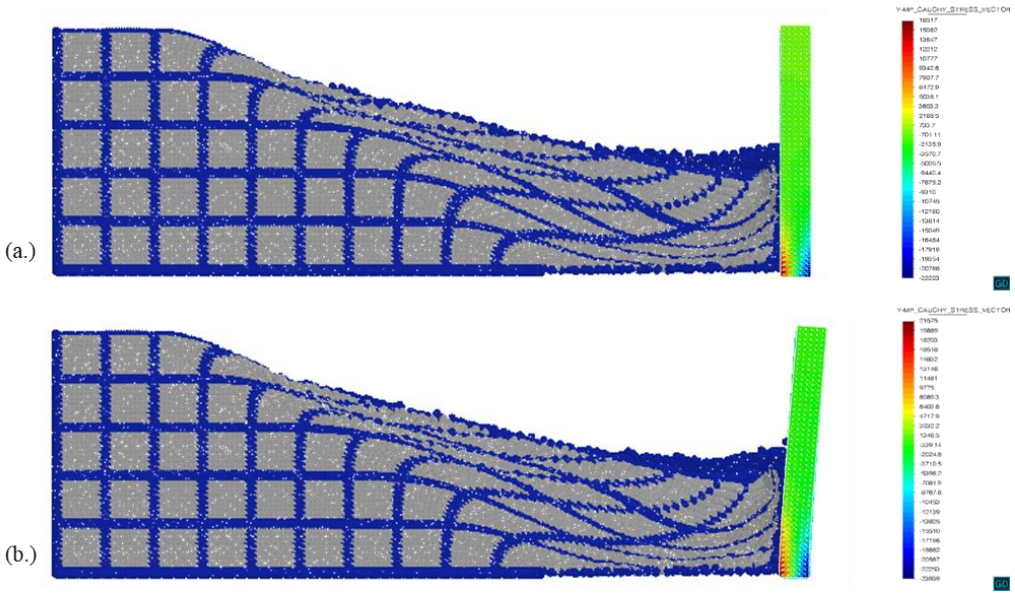

Figure 4 Deformed configuration of the soil-structure interaction tests of granular flow impacting (a) rigid and (b) flexible structure

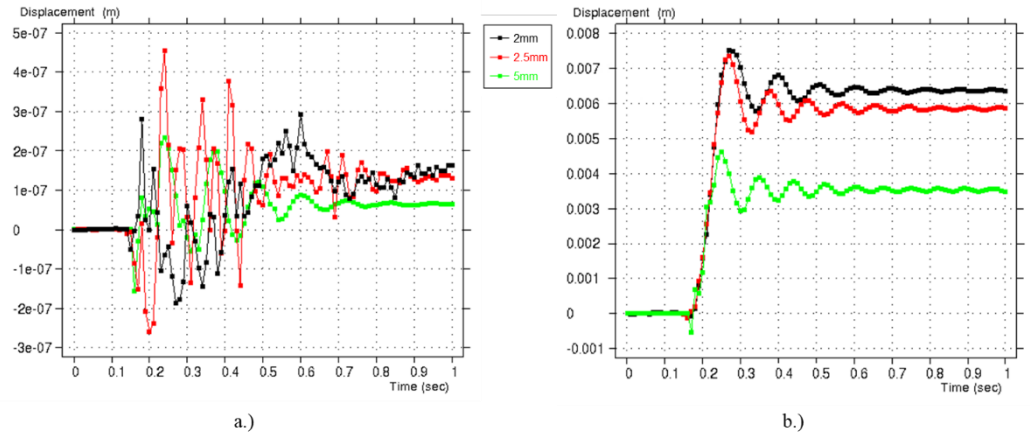

Figure 5 Displacement of (a) rigid and (b) flexible structure at point "A" upon impact and how it changes with respect to mesh refinement

CONCLUSIONS

A monolithic coupling scheme to simulate soil-structure interaction problems is presented in the current study. The formulation is implemented in an implicit approach of MPM as it is able to solve problems which involve transitioning from small to large deformations and displacements more accurately. Some simulation tests have been performed to validate and check the implemented formulations. Nevertheless, some future works are necessary to improve the accuracy and quality of the numerical results, such as by improving the soil and structural model or by investigating in details the contact-force and coupling scheme of the soil and the structural elements, before conducting a real-scale landslide simulation.

ACKNOWLEDGEMENTS

The research work was supported by CIMNE, particularly the Kratos-Multiphysics group under the leadership of Prof. Eugenio Oñate, and by Prof. Mitsuteru Asai and his group during the first author's two-month visit at Kyushu University. A grateful acknowledgment is also given to the Riken CCS, DAAD, Erasmus+ and the Bavarian Graduate School of Engineering (BGCE) for the valuable financial support during the research work was conducted.

REFERENCES

Andersen S. & Andersen L. (2010). Modelling of landslides with the material-point method. *Computational Geosciences*, 14(1): 137-147.

Bandara S & Soga K. (2015). Coupling of soil deformation and pore fluid flow using material point method. *Computers and Geotechnics*, 63: 199-214.

Bui HH, Fukagawa R, Sako K, & Ohno S. (2008). Lagrangian meshfree particles method (SPH) for large deformation and failure flows of geomaterial using elastic–plastic soil constitutive model. *International Journal for Numerical and Analytical Methods in Geomechanics*, 32(12): 1537-1570.

Clausen J, Damkilde L, & Andersen L. (2007). An efficient return algorithm for non-associated plasticity with linear yield criteria in principal stress space. *Computers & Structures*, 85(23-24): 1795-1807.

Dadvand P. (2007) *A framework for developing finite element codes for multi-disciplinary applications*, PhD thesis, Universidad Politécnica de Cataluña, Barcelona, Spain.

Dadvand P, Rossi R, & Oñate E. (2010). An object-oriented environment for developing finite element codes for multi-disciplinary applications. *Archives of computational methods in engineering*, 17(3): 253-297.

Fern EJ & Soga K. (2016). The role of constitutive models in MPM simulations of granular column collapses. *Acta Geotechnica*, 11(3): 659-678.

Goudie AS. (2006). Global warming and fluvial geomorphology. *Geomorphology*, *79*(3-4), 384-394.

Guilkey JE & Weiss JA. (2003). Implicit time integration for the material point method: Quantitative and algorithmic comparisons with the finite element method. *International Journal for Numerical Methods in Engineering*, 57(9): 1323-1338.

Harlow FH. (1964). The particle-in-cell computing method for fluid dynamics. *Methods for Computational Physics*, 3: 319-343.

Huang P, Zhang X, Ma S, & Wang HK. (2008). Shared memory OpenMP parallelization of explicit MPM and its application to hypervelocity impact. *CMES: Computer Modeling in Engineering & Sciences*, 38(2): 119-148.

Iaconeta I, Larese A, Rossi R, & Zhiming G. (2016). Comparison of a material point method and a Galerkin meshfree method for the simulation of cohesive-frictional materials. *Materials*, 10(10), p. 1150.
Iaconeta I, Larese A, Rossi R, & Oñate E. (2017). An implicit material point method applied to granular flows. *Procedia Engineering*, 175, 226-232.
Iaconeta I, Larese A, Rossi R, Oñate E. (2018) A stabilized, mixed, implicit Material Point Method for non-linear incompressible solid mechanics problems. *Submitted to Computational mechanics*.
Kundzewicz ZW, Kanae S, Seneviratne SI, Handmer J, Nicholls N, Peduzzi P., ... & Muir-Wood R. (2014). Flood risk and climate change: global and regional perspectives. *Hydrological Sciences Journal*, 59(1), 1-28.
Mast CM. (2013). *Modeling landslide-induced flow interactions with structures using the material point method*, PhD thesis, University of Washington, Seattle, Washington, United States of America.
Petley D. (2012). Global patterns of loss of life from landslides. *Geology*, *40*(10), 927-930.
Soga K, Alonso E, Yerro A, Kumar K, & Bandara S. (2015). Trends in large-deformation analysis of landslide mass movements with particular emphasis on the material point method. *Géotechnique*, 66(3): 248-273.
Sulsky D, Chen Z, & Schreyer HL. (1994). A particle method for history-dependent materials. *Computer methods in applied mechanics and engineering*, 118(1-2): 179-196.
Sulsky D, Zhou SJ, & Schreyer HL. (1995). Application of a particle-in-cell method to solid mechanics. *Computer physics communications*, 87(1-2): 236-252.
Wang B, Vardon PJ, Hicks MA, & Chen Z. (2016). Development of an implicit material point method for geotechnical applications. *Computers and Geotechnics*, 71: 159-167.
Zienkiewicz OC & Taylor RL. (1977). *The finite element method* (Vol. 36). London: McGraw-hill.